Title
FACTORS INFLUENCING THE ACCEPTANCE TIME OF FELIX

Authors
Garren, Alper A.
Hiskes, John R.
Smith, Lloyd.

Publication Date
1957-09-16

UNIVERSITY OF CALIFORNIA
Radiation Laboratory

DOCUMENT NUMBER UCRL-3939

Cover Sheet
Do Not Remove

~~RESTRICTED DATA~~

~~This document contains restricted data as defined in the~~ Atomic Energy Act of 1954 Its transmittal or the disclosure of its contents in any manner to an unauthorized person is prohibited.

INDEX NO. 4502-41 CV-1
This document contains 18 pages
This is copy 16 of 17 series A
Date 9-16-57

DECLASSIFIED

Issued to Info Div [illegible]

~~SECRET~~
Classification

Each person who receives this document must sign the cover sheet in the space below.

Route to	Noted by	Date	Route to	Noted by	Date

RL-1788(3/57)

DISCLAIMER

SECRET

UCRL-3939

RADIATION LABORATORY - UNIVERSITY OF CALIFORNIA - BERKELEY

ENGINEERING NOTE

JOB NUMBER	FILE NO.	PAGE
4502-41	CV-1	1

SUBJECT

FACTORS INFLUENCING THE ACCEPTANCE TIME OF FELIX

NAME see below *

DATE 16 September 1957

DECLASSIFIED

* by Alper A. Garren, John R. Hiskes and Lloyd Smith

DISTRIBUTION:

THIS DOCUMENT CONTAINS 18 PAGES.
THIS IS COPY 16 OF 17. SERIES A.

1/A - C. M. Van Atta, Berkeley
2/A - C. M. Van Atta, Livermore
3/A - Lloyd Smith
4/A - Information Division, Berkeley
5/A - Information Division, Livermore
6/A - Information Division, Livermore
7/A - Information Division, Livermore
8/A - Charles M. Carman, Patent Office, Livermore
9/A - Carl Backlund, AEC San Francisco
10/A - R. F. Post
11/A - W. A. S. Lamb
12/A - Frank S. Eby
13/A - Charles C. Damm
14/A - Ross E. Hester
15/A - Eugene J. Lauer
16/A - Ted Northrop
17/A - J. C. Kilpatrick

CLASSIFICATION CANCELLED (OR CHANGED TO Unclassified
(INSERT APPROPRIATE CLASSIFICATION)

BY AUTHORITY OF SAN AEC LTR DTD 9/17/58
(PERSON AUTHORIZING CHANGE IN CLASSIFICATION)

BY D. Lindholm 11-24-58
(SIGNATURE OF PERSON MAKING THE CHANGE, AND DATE THEREOF)

RESTRICTED DATA

This document contains restricted data as defined in the Atomic Energy Act of 1954 Its transmittal or the disclosure of its contents in any manner to an unauthorized person is prohibited.

46009

SECRET

RL-398

DECLASSIFIED

24 kg
20 kv

Actual 20 kg. 14.6 ms

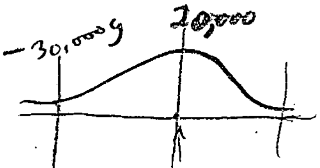

Field at this pt. assumed to reach 20,000 gauss in 4.8 m sec.

Full 20 kv on bank (unobtainable) gives 24,500 g at mirror peak

For $R = 1.5$

$$\frac{dH_z}{dt}\Big|_{t=0} = 6.55 \frac{\text{gauss}}{\mu s} \text{ at this point}$$

$$\frac{24,500}{1.5} \approx 16 \text{ kg}$$

$$\frac{dH_z}{dt}\Big|_{t=0} = \frac{6.55}{1-\alpha_i} \frac{\text{gauss}}{\mu s} \text{ at inflection point.}$$

$$(\text{For } \alpha = 0.2) = 8.20 \frac{\text{gauss}}{\mu s} \text{ at infl. pt.}$$

NAME: Garren, Hiskes + Smith
DATE: 16 September 1957

SUBJECT: FACTORS INFLUENCING THE ACCEPTANCE TIME OF FELIX

The purpose of this note is to present a theoretical estimate of the acceptance time in Felix, taking into account the non-adiabatic and precessional effects indicated by the orbit computations of the last several months. Our knowledge of these effects is by no means complete, the most obvious gap being complete ignorance of non-adiabatic effects in a time rising field, so that the following quantitative predictions should not be taken too literally. We guess that they are correct, probably well within a factor of two, but plan to test the most promising configurations by detailed orbit computations in the actual time varying Felix field.

Loss Cone and Clearance on First Turn

An absolute upper limit to the acceptance time for constant injection energy, regardless of how cleverly one may exploit precessional and jitter effects (see page 6), may be obtained by determining for given source position the maximum radius of curvature leading to orbits outside the true (non-adiabatic) loss cone, and the minimum radius of curvature required to miss the source on the first turn. Fig. 1 shows how these quantities depend on source position. The line marked "stable-unstable" marks the loss cone, and is derived from the machine computations at V = 0.6, 0.4, 0.2. The lower curves marked with various values of Δz are obtained from the adiabatic expression for displacement parallel to the field in one turn for injection perpendicular to the field lines:

$$\Delta z = -\pi^2 \rho^2 \frac{1}{H} \frac{dH}{dz} \qquad (1)$$

where ρ is the radius of curvature at the source and the derivative is with respect to the field direction at the source. All these curves really depend also on the radial position of the source and angle of injection in the x-y plane, but our impression is that the variation is not large.

The parameter V is uniquely related to the time at which the particle is injected by the formula:

$$V = \frac{2\pi}{L} v \frac{mc}{eH} = \frac{2\pi}{L} v \frac{mc}{eH_0 t} \sim \frac{160 \times 10^{-6}}{t} \qquad (2)$$

-- $H = H_0 t$ (H_0 at inj. pt.)

The numerical value is based on 10 kev deuterons, a rise of field at the center to 20,000 gauss in 4.8 msec and a length of 100 cm. Thus the earliest and latest injection times for given source position and extent of source structure to be cleared can be computed from the appropriate V_{max} and V_{min}. Table I gives these times for various source positions. It can be seen that the average effective time decreases gradually with increasing z.

Precessional Effects and Adiabatic Trapping

It should be realized that these phenomena can not be used to extend the times given in Table I, but rather serve to insure that a sizeable fraction of those times are indeed useful. There are three major points to consider here; clearing the source

---

~~1 Alfven, Cosmical Electrodynamics, pp. 21.~~

on the first transit, and clearing in z or r after a complete precession cycle. In order to discuss them, one needs a quantitative measure of precession. The solid curve of Fig. 2 is the adiabatic result; i.e., the integral of the lateral drift velocity[1] for one transit in the Felix field. The lettered points represent the corresponding numbers available from the exact orbit computations. It can be seen that the adiabatic approximation represents the truth moderately well, and accordingly we have chosen to represent the precession per transit by a straight line approximation.

$$\Delta\theta(\mathrm{rad}) = V[1.66 - 0.044z\ (\mathrm{cm})] \qquad (3)$$

The precession undoubtedly depends also on the radial position of the guiding center, but the one exact orbit we have following a different flux tube shows a precession falling within the scatter of the other points in Fig. 2. Since the adiabatic calculation also indicates only a weak dependence, we shall adopt (3) as an adequate representation for present purposes.

Regarding the problem of missing the source on the first transit (see Fig. 3 for geometrical arrangement), we neglect the effect of the time varying field and rely on precession only. Since the axial distance covered by an ion during the last half turn at reflection is generally small, we assume that it will hit the source if the projected circle in the x-y plane, after one transit, intersects the small circle representing the source. Analyzing the geometry of the two circles, one arrives at the following requirement for the precession angle:

$$\Delta\theta > \frac{\rho \sin\gamma}{R_s - \rho\cos\gamma}\left\{\left[1 + \frac{2a}{R_s\rho}\,\frac{R_s - \rho\cos\gamma}{\sin^2\gamma}\right]^{1/2} - 1\right\} \qquad (4)$$

where ρ = radius of projected circle at the source

R_s = radial position of the source

a = radius of the source

γ = angle of injection measured outward from the azimuthal direction.

Since $\rho \sim (L/2\pi)V$, Eqs. (3) and (4) determine a maximum permissible z for the source* as a function of V and the angle, γ, such that the precession be sufficient to insure missing on the first transit. The right-hand set of curves in Fig. 1, marked with values of γ, give this upper bound for a = 1/4 inch, R_s = 17.5 cm. That the limiting z increases with γ results from the fact that the source is easier to miss if the ions are projected outward.

---

[1] Alfven, Cosmical Electrodynamics, pp. 21.

* Beyond z = 1.66/0.044 = 38 cm, the precession reverses and the consequences are different, but the interesting region for injection seems to be well within this point.

DECLASSIFIED

Before discussing the significance of these limiting curves, we proceed to the adiabatic decrease in z and r after precession through an angle $2\pi/N$, N indicating either the number of sources at the same r and z, or the reciprocal of the number of 360^o precessions if more than one is allowed. Under the assumption of adiabaticity, the two expressions are:

$$\delta z = \frac{2\pi}{N\Delta\theta}\frac{4}{vt}\frac{1}{\left(\frac{1}{H}\frac{dH}{dz}\right)_s}\int_0^{z_s} dz\sqrt{1 - \frac{H(z,r)}{H(z_s,r_s)}} \qquad (5)$$

and

$$\frac{\delta r}{r} = \frac{2\pi}{N\Delta\theta}\frac{2}{vt}\int_0^{z_s}\frac{dz}{\sqrt{1 - \frac{H(z,r)}{H(z_s,r_s)}}} \qquad (6)$$

where the subscript, s, refers to source position.

For H varying as $[1 - \alpha \cos(2\pi z/L)]$, (ignoring the variation in radius of the position of the guiding center) Eqs. (5) and (6) are expressible in terms of elliptic integrals. It may, incidentally, be verified that (5) agrees with the expression given by Post for a uniform field terminated by short mirrors. With the addition of the precession factor, the expressions take on a new meaning, however. The shrinkage per transit depends on the fractional change in H per transit and is thus inversely proportional to the field magnitude at injection and thus to the time at injection, t. On the other hand, the precession per transit by (2) and (3) decreases inversely as the injection time, t, for constant injection energy. As a result, by the time the orbit has precessed through a large angle, $2\pi/N$, the total shrinkage is independent of injection time, but only depends on the axial position of the injector, which appears explicitly in (3), (5) and (6). One then concludes that the adiabatic shrinkage, which once determined an injection time, determines rather a minimum z for the source depending only on the size of the source structure.

Integrating (5) and introducing (3) and (2) leads to the condition on source location to miss in z for N = 1;

$$\delta z\ (cm)\left[\frac{53}{z_s(cm)} - 1.40\right] < \frac{4}{\pi}\frac{E(\sin x) - \cos^2 x\, K(\sin x)}{x \sin x \cos x} \qquad (7)$$

where $x = (\pi z_s/L)$, δz = length of source inward from point of injection, and K and E are the complete elliptic integrals of first and second kind. The solution of (7) is represented by the vertical lines in Fig. 1.

Similarly, from (6), for N = 1

$$z_s\ (cm) > 36 - 0.87\ (R_s/\delta r)K(\sin x) \qquad (8)$$

in order to miss in r.

δr is not simply the radius of the source, for if the ions are projected outward in the x-y plane, the outer edge of the circle must move in to pass under the source after precession. Here the geometry gives the required δr:

$$\delta r = \rho \left[1 - \frac{R_s \cos \gamma - \rho}{(\rho^2 + R_s{}^2 - 2\rho R_s \cos \gamma)^{1/2}} \right] + a \qquad (9)$$

Combining (8) and (9), we obtain a new family of curves of minimum allowable z as a function of V for various angles of injection, γ. These curves appear at the left side of Fig. 1. (R_s = 17.5 cm, a = 1/4 inch.)

Use of Fig. 1

Since Fig. 1 in its completeness consists of a somewhat confusing maze of curves to be interpreted in different ways, we shall attempt to summarize the argument up to this point before proceeding further. There are 5 types of curves:

(1) A single, almost straight line of negative slope marking the boundary of the non-adiabatic loss cone. Particles injected with values of V above this line will run out of the mirror or strike the source after relatively few transits.

(2) A set of curves, concave upwards, characterized by the Δz required to miss the source on the first turn. Particles injected perpendicular to the field direction at distance Δz from the leading edge of the source will strike the source on the first turn if V falls below the corresponding curve.

(3) The set of lines on the right characterized by the injection angle, γ, in the x-y plane, expressing the restriction imposed by asking that the particles miss the source on the first transit by virtue of precession. Particles injected below and to the right of the appropriate γ-curve will strike on the first transit.

(4) The set of vertical lines characterized by the required shrinkage, δz, to miss the source axially after 360° precession. Particles injected to the left of these curves will fail to clear in z after 360° precession.

(5) The set of curves to the left, characterized by γ, representing the restriction of missing the source radially after 360° precession. Particles injected to the left of these curves will fail to clear in radius after 360° precession.

Acceptance time for given Δz = δz, given γ and given axial source position, is obtained by reading from Fig. 1 the minimum and maximum values of V permitted by the interlacing five curves, and translating to time by the use of expression (2). It must be remembered that only the less restrictive of (4) and (5) need be considered, for if the ion clears axially its radial position does not matter and vice versa. In this manner we arrive at Table II, giving the earliest and latest injection times and the differences for various source positions and values of γ and Δz = δz.

For a source injecting over a range of ± 20° in γ it would appear that the optimum occurs at about z = 20 cm with the source oriented to give an average outward angle of about 20°. It would also appear that the rear half of the source is not very effective; if, for instance, neutral gas accompanying the ion current presents a serious problem one might just as well block off the rear half of the source. One can also extract an effective injection time from Table II, that is a time which, when multiplied by the total source current, gives the total injected charge. At an axial source position of 20 cm this is about 300 μsec for optimum average γ, tapering off to about 200 μsec at 15 and 25 cm. The 200 μsec figure is more uncertain, for the optimum orientation appears to involve values of γ beyond the range of Fig. 1.

Effect of Injecting at an Angle to the Normal to the Field

The foregoing numerical work is based on injection normal to the field lines. Apparently not much is known about the source distribution in angle except that the ends of beam fan out to about 15°. On the suspicion that an initial angle in the (r,z) plane may be quite important, we repeated the analysis for the particular cases projecting 5° forward at $\Delta z = 1$ cm and 5° backward at $\Delta z = 3$ cm. The backward moving ion is essentially useless. For the forward moving one, however, there is a great increase in available time in the range of source positions for which the ions clear the source radially after precession. Table III is Table II recomputed for this special case. It can be seen that the effect of an angle is indeed great; if we assume that those numbers represent an average for the front end of the source and there is no contribution from the back end, the effective time is about 700 μsec. This is made possible by the fact that ions can miss the source radially even though the excursions in z remain large. It should be pointed out, however, that the injection period ends at close to half peak field, so that after compression the plasma would be about 10 cm in radius with many particles at only 20 kv energy.

Jitter

A non-adiabatic effect of some interest is the fact that even in a static field the ions do not always reflect at the same value of z and radial position of the guiding center. The true z_{max} is related to the phase of the ion in its circular path at reflection,* and since this phase varies greatly from one transit to the next, the successive values of z_{max} vary in a somewhat chaotic fashion; thus the name "jitter". It can be beneficial in permitting a certain number of border line cases to survive or harmful in cutting out others which would have been safe otherwise. We have examined the magnitude of the effect for a few cases in the interesting range: for $V = 0.4$, the overall variation in z is 2 cm at a z of 20 cm, decreasing to 0.6 cm at a z of 6 cm, while at $V = 0.2$ the variation is negligibly small. Since the source will lie on a flux line the jitter should not have much effect on the radial separation of the orbit and the source at successive reflections. For most times of interest the jitter effect is probably small; we have not attempted to explore it further.

Change in Injection Energy and Rate of Field Rise

Using a different (but constant) injection energy changes the preceding arguments in two ways. Increasing the energy to produce the same orbits at later times increases the acceptance times of Table I proportionally. On the other hand, the precession

---

* As a rule, z_{max} is greatest when the particle reflects at the point of its circle farthest from the axis. Also all reflections occur fairly near this phase.

per transit is the same for the same geometrical orbit, but the shrinkage in r and z per transit decreases because the time per transit decreases and simultaneously the magnetic field is greater in magnitude. As a result, the precessional curves in Fig. 1 bounding the useful area on the left will move to the right, further restricting the useful area. We have not attempted any quantitative analysis at a different energy, but a comparison of Tables I and II shows that at 10 kv the precessional curves limit the acceptance times somewhat, though not drastically, over a considerable range in z. We guess, therefore, that the competing effects are rather well balanced at 10 kv, and there is probably not much to be gained in total accepted charge by going higher or lower.

A similar argument applies to the rate of rise of magnetic field. A slower rise would increase the times of Table I proportionally, but the shrinkage per transit decreases and the left-hand bounding curves again move to the right. Therefore we again conclude that, everything else (such as charge exchange) neglected, there is probably not much to gain by changing the rate of rise.

Variable Injection Energy

It also does not look as though there is much to be gained by programming the injection energy. The reason is seen most strikingly in Table III. Injection begins at about 400 μsec, lasting to 2000 μsec in the most favorable case. If 10 kv or so is the peak voltage to be considered, the best one could hope for would be to utilize the first 400 μsec with an increase in total charge of 400/1600 = 25%. Moreover, if charge exchange is important, the ions of low initial energy are susceptible for the longest time. Finally, according to the adiabatic compression laws, the early ions would actually lower the average energy of the final distribution, though they would be concentrated more densely.

The figures in Table III represent an extreme case, but a look at all the tables shows that where there is a decent acceptance time at 10 kv, filling earlier times by programming will not increase total charge by more than a factor of two.

Multiple Sources

It is not clear that one can gain appreciably in total charge by introducing more sources. Referring to Fig. 1, the left-hand bounding curves move to the right as the total allowed precession decreases from 360°. For two sources 180° apart, the $\delta z = 1$ cm boundary moves to the position of the $\delta z = 2$ cm curve, and so on. The $\gamma = 0$ curve for radial shrinkage moves out to 20 cm. This leaves some area available, but not much. On the basis of such a crude estimate we are sure that the total acceptable charge is certainly less than proportional to the number of sources, perhaps even decreasing as more structures are inserted. However, we would prefer to see whether the considerations of one source are corroborated by experience with Felix before attempting to predict the multiple source case.

One could also introduce a second source at such a position in r and z that it does not interfere with the trajectories from the first source and vice versa. This procedure seems to us less likely to be harmful, but if the first source is in optimum position, the second will not contribute as much.

β, Thermalization, Neutron Production

If we adopt the largest of the various computed acceptance times, 700 μsec, and a source current of 1/6 amp, the total number of injected particles is 7×10^{14}. The volume after compression for this case is 1.5×10^4 cm^3, giving a density of 4×10^{10} and an average energy of 35 kv (ranging from 15 to 80 kv). The thermalizing time[2] is 30 sec; the dependence of this time on the various parameters of the system is not great enough to change this time downward by an order of magnitude, so that one can to the first approximation ignore the effect of Coulomb collisions on the ion orbits for 100 msec or so.

In this case β does not mean much, for there is really no temperature to the system. Nevertheless, $n\bar{W}/(B^2/8\pi) \sim 10^{-4}$, which is still a rough measure of the "loading" of the containing field.

Neutron production is still harder to predict, for $\overline{\sigma v}$ depends strongly on the way in which the various compressed orbits intersect each other. Having nothing better to go by, we adopt $\overline{\sigma v} = 10^{-17}$ (temperature of 50 kv); this yields the result

$$\frac{dN}{dt} = 2 \times 10^5/\text{millisecond}$$

One might as reasonably estimate yield by assuming, for instance, that 10% of the ions have 80 kv energy and the rest are effectively standing still. On this basis the yield is $\sim 10^4$/millisecond.

The yields are expressed as rates to avoid the question of loss during and after compression due to charge exchange. The presence of neutrals can be quite serious; at a neutral density of 10^{10} (10^{-7} mm) the lifetime against charge exchange would not be more than a few milliseconds.

Concluding Remarks

It would appear that the rate of rise of field and injection energy have been well chosen to optimize the total trapped charge. Any substantial improvement would have to come from an increase in injected current, resulting in a linear increase of charge and β, and a quadratic increase in neutron yield. Since the neutron yield is a sensitive function of ion energy and the geometry of the intersecting orbits, it might be profitable to examine a variety of situations, also including the use of multiple sources and programmed voltages, in an effort to determine ways of optimizing yield without regard to total charge and β. Fig. 1 is probably not sufficiently flexible for such a study, and we have therefore included an appendix containing the formulas required for a more general description of the injection process.

---

[2] Spitzer, Physics of Fully Ionized Gases, page 78.

Table I

Maximum injection times (μsec) limited only by stability and first turn clearance.
z = axial distance from machine center to end of source.
Δz = axial distance from end of source to source point considered.

Δz (cm)	V_f	V_i	t_f	t_i	Δt	$(\Delta t)_{av}$
			z = 10 cm			
1	0.170	0.570	940	280	660	
2	0.237	0.555	680	290	390	440 μsec
3	0.285	0.537	560	300	260	
			z = 15 cm			
1	0.1625	0.495	980	320	660	
2	0.230	0.482	700	330	370	420 μsec
3	0.282	0.470	570	340	230	
			z = 20 cm			
1	0.1675	0.432	960	370	590	
2	0.238	0.420	670	380	290	340 μsec
3	0.297	0.407	540	390	150	
			z = 25 cm			
1	0.180	0.365	890	440	450	
2	0.260	0.355	620	450	170	210 μsec
3	0.327	0.342	490	470	20	
			z = 30 cm			
1	0.205	0.302	780	530	250	80 μsec
2	-	-	-	-	-	
3	-	-	-	-	-	

Table II

Injection Times limited by first turn clearance, stability, first transit precessional clearance, and axial or radial adiabatic shrinkage in one precessional period--as a function of z, Δz and γ, the transverse injection angle measured outward from the azimuthal direction.

	γ	V_f	V_i	t_f	t_i	Δt	$(\Delta t)_{av}$ (over γ)
				z = 10 cm			
Δz = 1 cm	0	0.170	0.570	940	280	660	
	10	0.170	0.292	940	550	390	
	20	--	--	--	--	--	
	30	--	--	--	--	--	
	40	--	--	--	--	--	180
Δz = 2 cm	0	0.237	0.555	670	290	380	
	10	0.237	0.342	670	470	200	
	20	--	--	--	--	--	
	30	--	--	--	--	--	
	40	--	--	--	--	--	100
Δz = 3 cm	0	0.285	0.537	560	300	260	
	10	0.285	0.384	560	420	140	
	20	--	--	--	--	--	
	30	--	--	--	--	--	
	40	--	--	--	--	--	70
					Average (over Δz)		120 μsec
				z = 15 cm			
Δz = 1 cm	0	0.1625	0.495	980	320	660	
	10	0.1625	0.495	980	320	660	
	20	0.1625	0.232	980	690	290	
	30	--	--	--	--	--	
	40	--	--	--	--	--	320
Δz = 2 cm	0	0.230	0.482	700	330	370	
	10	0.230	0.482	700	330	370	
	20	0.230	0.257	700	620	80	
	30	--	--	--	--	--	
	40	--	--	--	--	--	160
Δz = 3 cm	0	0.282	0.470	570	340	230	
	10	0.282	0.470	570	340	230	
	20	0.282	0.285	570	560	10	
	30	--	--	--	--	--	
	40	--	--	--	--	--	90
					Average		190 μsec

Table II (cont.)

	γ	V_f	V_i	t_f	t_i	Δt	$(\Delta t)_{av}$ (over γ)
			$z = 20$ cm				
$\Delta z = 1$ cm	0	0.1675	0.432	960	370	590	
	10	0.1675	0.432	960	370	590	
	20	0.1675	0.432	960	370	590	
	30	0.1675	0.432	960	370	590	
	40	0.1675	0.432	960	370	590	590
$\Delta z = 2$ cm	0	0.238	0.420	670	380	290	
	10	0.238	0.420	670	380	290	
	20	0.238	0.420	670	380	290	
	30	0.238	0.280	670	570	100	
	40	—	—	—	—	—	210
$\Delta z = 3$ cm	0	0.297	0.407	540	390	150	
	10	0.297	0.407	540	390	150	
	20	0.297	0.407	540	390	150	
	30	0.297	0.308	540	520	20	100
	40	—	—	—	Average	—	300 μsec
			$z = 25$ cm				
$\Delta z = 1$ cm	0	—	—	—	—	—	
	10	0.180	0.365	890	440	450	
	20	0.180	0.365	890	440	450	
	30	0.180	0.365	890	440	450	
	40	0.180	0.365	890	440	450	450
$\Delta z = 2$ cm	0	—	—	—	—	—	
	10	0.260	0.355	620	450	170	
	20	0.260	0.355	620	450	170	
	30	0.260	0.355	620	450	170	
	40	0.260	0.355	620	450	170	170
$\Delta z = 3$ cm	0	—	—	—	—	—	
	10	0.327	0.342	490	470	20	
	20	0.327	0.342	490	470	20	
	30	0.327	0.342	490	470	20	
	40	0.327	0.342	490	470	20	20
					Average		210 μsec

Table II (cont.)

	γ	V_f	V_i	t_f	t_i	Δt	$(\Delta t)_{av}$ (over γ)
				z = 30 cm			
Δz = 1 cm	0	—	—	—	—	—	
	10	—	—	—	—	—	
	20	0.263	0.302	610	530	80	
	30	0.210	0.302	760	530	230	
	40	0.203	0.302	790	530	260	180
Δz = 2 cm	0						
	10						
	20						
	30						
	40						0
Δz = 3 cm	0						
	10						
	20						
	30						
	40						0
					Average		60 µsec

RADIATION LABORATORY - UNIVERSITY OF CALIFORNIA - BERKELEY

ENGINEERING NOTE

JOB NUMBER	FILE NO	PAGE
4502-41	CV-1	13

SUBJECT: FACTORS INFLUENCING THE ACCEPTANCE TIME OF FELIX

NAME: Garren, Hiskes + Smith

DATE: 16 September 1957

Table III

Same as Table II except all figures refer to Δz = 1 cm, ions injected 5° foreward from normal to flux line. This is taken as representative of front half of source, the back half contributing nothing since ions are presumed to be injected backwards there.

	γ	V_f	V_i	t_f	t_i	Δt	$(\Delta t)_{av}$
z = 10 cm	0	0.070	0.570	2280	280	2000	
	10	0.070	0.295	2280	540	1740	
	20	0.070	0.105	2280	1520	760	
	30	—	—	—	—	—	
	40	—	—	—	—	—	440 μsec
z = 15 cm	0	0.082	0.495	1950	320	1630	
	10	0.075	0.495	2140	320	1820	
	20	0.075	0.252	2140	690	1450	
	30	0.075	0.140	2140	1140	1000	
	40	0.075	0.090	2140	1780	360	660
z = 20 cm	0	0.137	0.432	1170	370	800	
	10	0.090	0.432	1780	370	1410	
	20	0.077	0.387	2080	410	1670	
	30	0.077	0.255	2080	630	1450	
	40	0.077	0.202	2080	790	1290	700
z = 25 cm	0	—	—	—	—	—	
	10	0.170	0.367	940	440	500	
	20	0.115	0.367	1400	440	960	
	30	0.095	0.367	1680	440	1240	
	40	0.087	0.367	1840	440	1400	425
z = 30 cm	0	—	—	—	—	—	
	10	—	—	—	—	—	
	20	0.262	0.302	610	530	80	
	30	0.210	0.302	760	530	230	
	40	0.157	0.302	1020	530	490	70

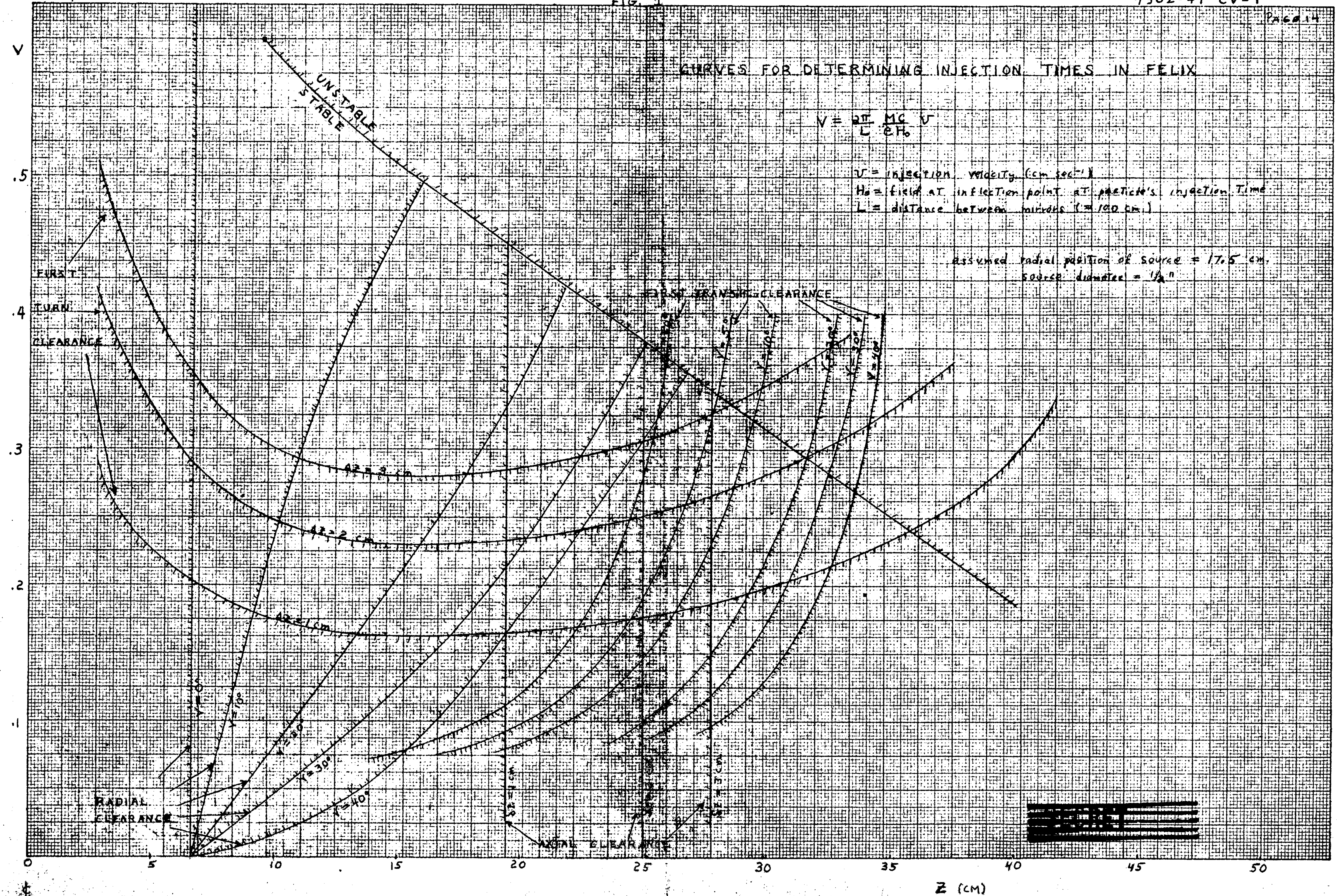
FIG. 1
Page 14
CURVES FOR DETERMINING INJECTION TIMES IN FELIX
V = 2π/L MC/eH₀ v
v = injection velocity (cm sec⁻¹)
H₀ = field at inflection point at particle's injection time
L = distance between mirrors (= 100 cm)
assumed radial position of source = 17.5 cm.
source diameter = 1/2"
UNSTABLE
STABLE
FIRST TURN CLEARANCE
FIRST TRANSIT CLEARANCE
RADIAL CLEARANCE
AXIAL CLEARANCE
V
.5
.4
.3
.2
.1
0
5
10
15
20
25
30
35
40
45
50
Z (CM)

[redacted]

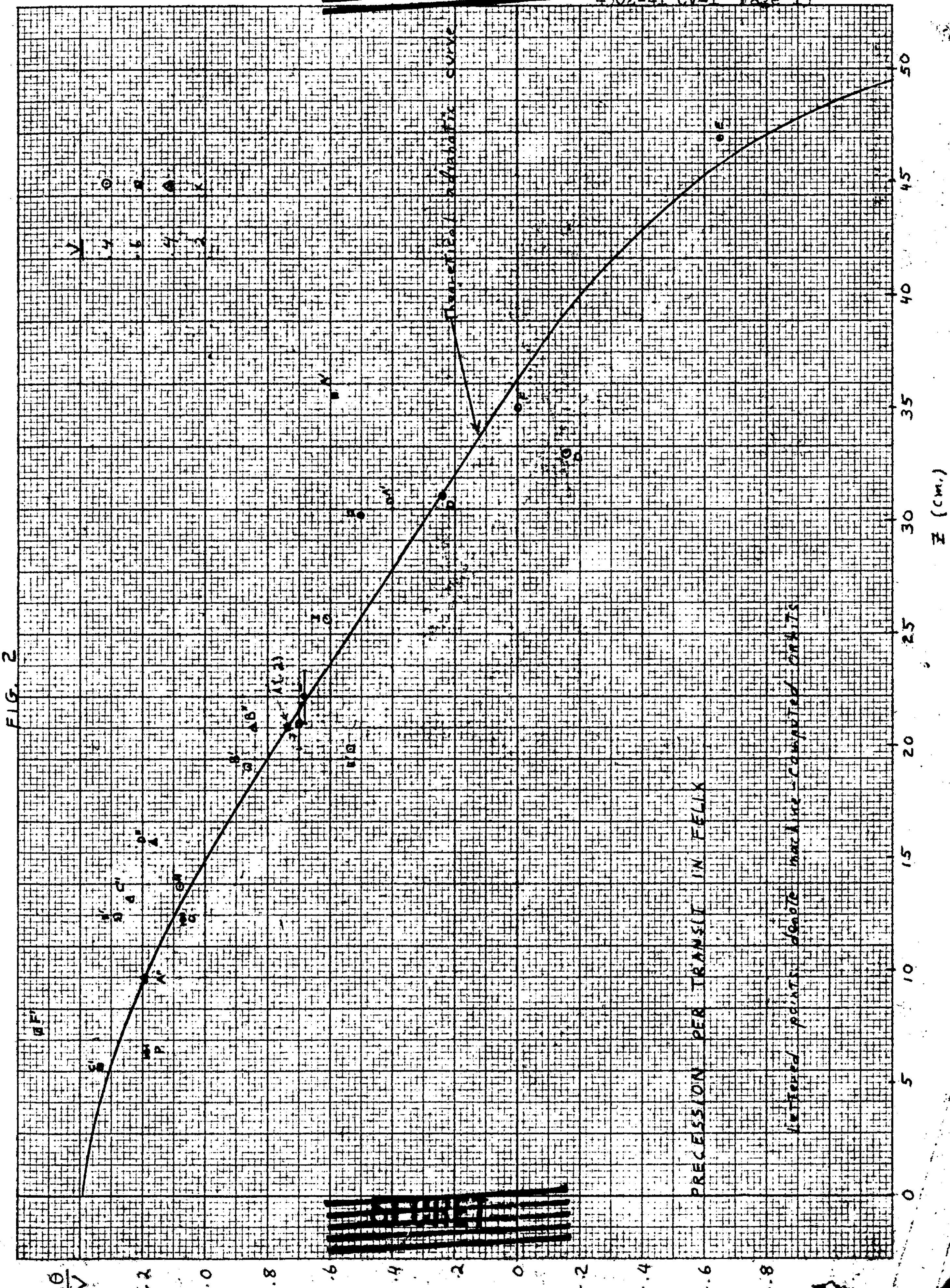

FIG. 2

[redacted]

K+E 10 X 10 TO THE ½ INCH 359-11 KEUFFEL & ESSER CO. MADE IN U.S.A.

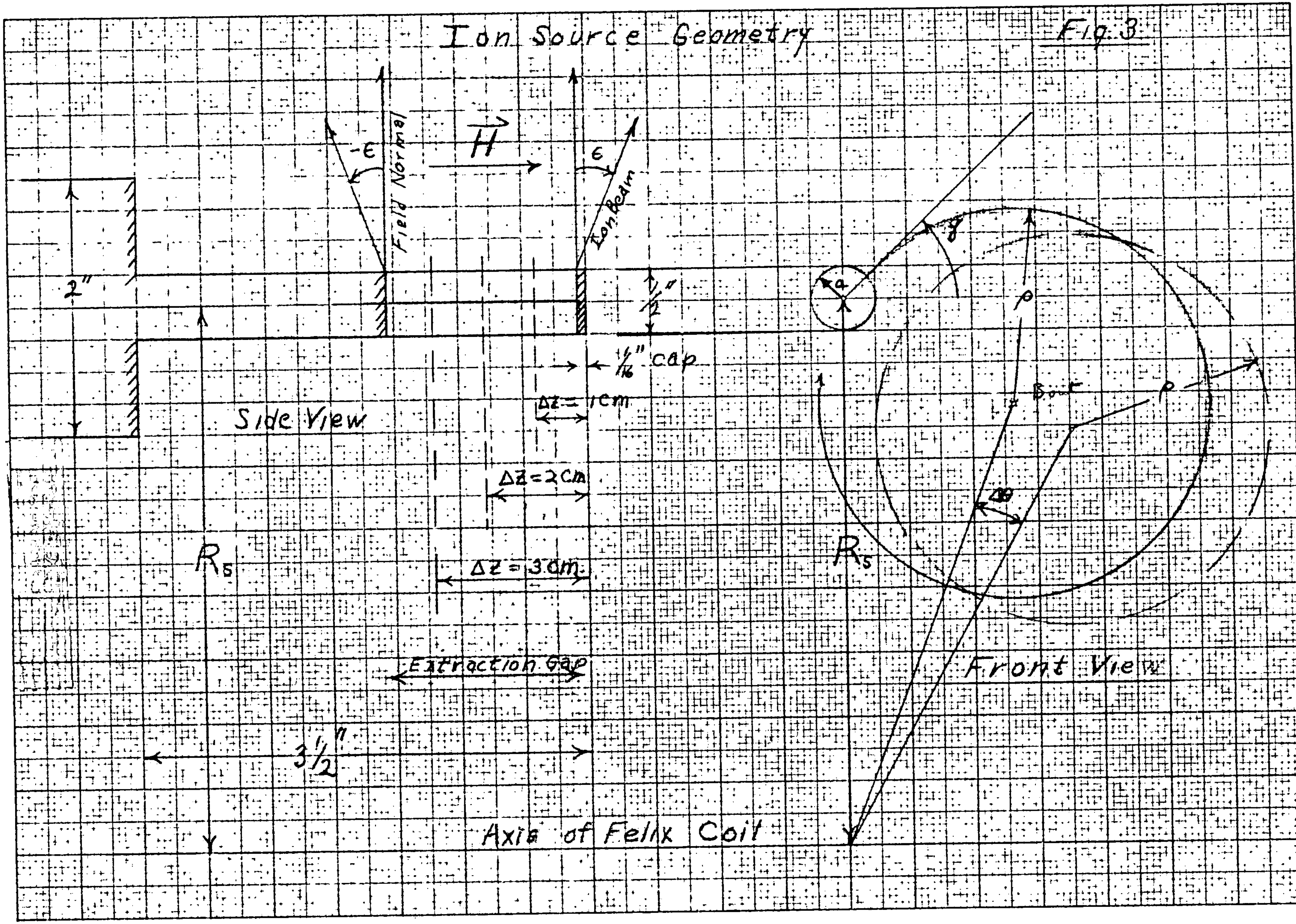
Ion Source Geometry
Fig. 3
Field Normal
Ion Beam
H
1/2"
1/16" cap
Δz = 1cm
Δz = 2cm
Δz = 3cm
Side View
2"
R5
Extraction Gap
3 1/2"
Axis of Felix Coil
Rs
Front View

APPENDIX: Summary of Formulas

(1) Precession

Precession angle per transit, using adiabatic approximation:

$$\Delta\theta = \frac{2Mcv}{e}\int_0^{z_s} \frac{\frac{1}{Hr}\frac{dH}{dr}}{\sqrt{H_s(H_s - H)}}\, dz$$

in field $H = H_0\left[1 - \alpha\cos\frac{2\pi z}{L}\, I_0\left(\frac{2\pi r}{L}\right)\right]$, taking field on axis, and replacing $\frac{1}{Hr}\frac{dH}{dr}$ by $\frac{1}{H_s r}\frac{dH}{dr}$:

$$\Delta\theta = \sqrt{2\alpha}\, V \frac{2E(\sin\frac{\pi z_s}{L}) - K(\sin\frac{\pi z_s}{L})}{(1 - \alpha\cos\frac{2\pi z_s}{L})^{3/2}}$$

(2) Axial Shrinkage--adiabatic--per transit

$$\delta_1 z = -\frac{4}{vt}\frac{1}{\frac{1}{H_s}\frac{dH_s}{dz}}\int_0^{z_s}\sqrt{1 - \frac{H}{H_s}}\, dz$$

or in field defined in (1)

$$\frac{\delta_1 z}{z_s} \approx \sqrt{2\alpha\frac{\overline{I_0}}{I_0(\frac{2\pi r_s}{L})}}\;{}^2\,\frac{L}{2vt}\cdot\frac{4}{\pi}\,\frac{E(\sin\frac{\pi z_s}{L}) - \cos^2\frac{\pi z_s}{L}K(\sin\frac{\pi z_s}{L})}{\frac{\pi z_s}{L}\sin\frac{\pi z_s}{L}\cos\frac{\pi z_s}{L}}$$

(3) Radial Shrinkage--adiabatic--per transit

$$\frac{\delta_1 r}{r} = \frac{1}{2}\frac{\delta H}{H} = \frac{1}{2}\frac{\Delta t}{t} = \frac{2}{vt}\int_0^{z_s}\frac{dz}{\sqrt{1 - \frac{H}{H_s}}}$$

$$\approx \frac{2}{vt}\sqrt{\frac{2(1 - \alpha\cos\frac{2\pi z_s}{L}\, I_0(\frac{2\pi r_s}{L}))}{\alpha I_0(\frac{2\pi}{L} r_s) - V))}}\, K(\sin\frac{\pi z_s}{L})$$

RL-398

RADIATION LABORATORY — UNIVERSITY OF CALIFORNIA — BERKELEY

ENGINEERING NOTE

JOB NUMBER	FILE NO.	PAGE
4502-41	CV-1	18

SUBJECT: FACTORS INFLUENCING THE ACCEPTANCE TIME OF FELIX

NAME: Garren, Hiskes + Smith

DATE: 16 September 1957

(4) Allowed Number of Transits to Accomplish δz or δr:

$\frac{2\pi}{\Delta\theta}\frac{1}{N}$, so

$$\delta r = \frac{2\pi}{N\Delta\theta}\,\delta_1 r$$

$$\delta z = \frac{2\pi}{N\Delta\theta}\,\delta_1 z - \frac{L}{2\pi}\,\frac{1 - \alpha\cos\frac{2\pi z_s}{L}}{\alpha\sin\frac{2\pi z_s}{L}}\,\epsilon^2$$ (cf. (5) for definition of ϵ)

(5) Axial Motion in First Turn after Injection

$$\Delta z = -\pi^2\rho^2\,\frac{1}{H}\frac{dH}{dz} + 2\pi\rho\epsilon$$

ρ = radius of curvature
ϵ = (axial angle of inclination to field line) - $\pi/2$

in field described in (1)

$$\Delta z \cong \frac{\pi}{2}\,\frac{L\alpha V^2\sin\frac{2\pi z_s}{L}}{\left(1 - \alpha\cos\frac{2\pi z_s}{L}\right)^3} + \frac{LV\epsilon}{\left(1 - \alpha\cos\frac{2\pi z_s}{L}\right)}$$

RL-398

SECRET

RESTRICTED DATA

This document contains restricted data as defined in the Atomic Energy Act of 1954. Its transmittal or the disclosure of its contents in any manner to an unauthorized person is prohibited.

SECRET